Slip flow in graphene nanochannels

Sridhar Kumar Kannam,[1,a)] B. D. Todd,[1,b)] J. S. Hansen,[2,c)] and Peter J. Daivis[3,d)]
[1]*Mathematics, Faculty of Engineering and Industrial Sciences and Centre for Molecular Simulation, Swinburne University of Technology, Melbourne, Victoria 3122, Australia*
[2]*DNRF Center "Glass and Time", IMFUFA, Department of Science, Systems and Models, Roskilde University, DK-4000 Roskilde, Denmark*
[3]*School of Applied Sciences, RMIT University, Melbourne, Victoria 3001, Australia*

(Received 5 July 2011; accepted 19 September 2011; published online 11 October 2011)

We investigate the hydrodynamic boundary condition for simple nanofluidic systems such as argon and methane flowing in graphene nanochannels using equilibrium molecular dynamics simulations (EMD) in conjunction with our recently proposed method [J. S. Hansen, B. D. Todd, and P. J. Daivis, Phys. Rev. E **84**, 016313 (2011)]. We first calculate the fluid-graphene interfacial friction coefficient, from which we can predict the slip length and the average velocity of the first fluid layer close to the wall (referred to as the slip velocity). Using direct nonequilibrium molecular dynamics simulations (NEMD) we then calculate the slip length and slip velocity from the streaming velocity profiles in Poiseuille and Couette flows. The slip lengths and slip velocities from the NEMD simulations are found to be in excellent agreement with our EMD predictions. Our EMD method therefore enables one to directly calculate this intrinsic friction coefficient between fluid and solid and the slip length for a given fluid and solid, which is otherwise tedious to calculate using direct NEMD simulations at low pressure gradients or shear rates. The advantages of the EMD method over the NEMD method to calculate the slip lengths/flow rates for nanofluidic systems are discussed, and we finally examine the dynamic behaviour of slip due to an externally applied field and shear rate. © *2011 American Institute of Physics*. [doi:10.1063/1.3648049]

I. INTRODUCTION

Transport of fluid at the nanoscale is very important in the design and fabrication of nanofluidic devices such as nanopumps, micro/nanoelectro mechanical systems (MEMS/NEMS), nanobiosensors, nanoreactors, nanoactuators, nanoengines, and lab-on-a-chip.[2–5] These devices have many potential applications such as water desalination, molecular computing, lubrication, drug delivery, fuel storage, mixing, and separation to name a few. Apart from these applications, the study of nanofluidics elucidates our understanding of the fluid behaviour in biological channels such as proteins and aquaporins, water flow in plants, soil science, and geology, all of which involves flow in nanometric pores. Reviews on nanofluidic phenomena and applications can be found in Refs. 2–5.

In order for these applications to become a commercial reality, we need to understand the fundamental behaviour of fluids confined to the nanoscale from a theoretical point of view in order to precisely control and manipulate fluids in applications. When fluids are confined to channel widths of only a few molecular diameters, the well established classical hydrodynamic theories based on the Navier-Stokes equations may fail,[6,7] and the no-slip boundary condition may no longer be valid.[8] Experimentally we still have to overcome certain limitations on probing and controlling molecules at the nanoscale.[9] Computer simulations, where we can model molecules explicitly, can be considered as the bridge between experiments and theory, and are playing an increasing role in our understanding of nanofluidic behaviour.[10,11] This is a very complex problem, as many properties of fluids change and new phase transitions are observed when they are confined in very narrow channels.[12] At the nanoscale, new physical constraints due to the matching of the hydrodynamic length scale with the dimension of the confinement length, alter the fluid behaviour. Also, in nanoscale systems, the surface to volume ratio becomes very high, so the interfacial effects become very important. Finally, in nanoscale systems confining walls induce strong density oscillations of the fluid across the channel so the fluid becomes highly inhomogeneous and as a result transport properties of the fluid become nonlocal in nature.[13,14] The influence of the surface and finite size effects on fluid transport needs therefore to be understood in detail, while such effects may be largely neglected for fluid flows in macroscopic channels.

II. THE SLIP BOUNDARY CONDITION

Over the last two centuries, many scientists including Bernoulli, Coulomb, Navier, Couette, Poission, Stokes, Poiseuille, Hagen, Helmholtz, and Maxwell have worked on formulating appropriate hydrodynamic boundary conditions at a fluid-solid interface.[15] Traditionally we assume the no-slip boundary condition to be valid, according to which the tangential velocity of the fluid relative to the adjacent solid is zero. Here we note that the assumption of a no-slip

a)Electronic mail: urssrisri@gmail.com.
b)Electronic mail: btodd@swin.edu.au.
c)Electronic mail: jschmidt@ruc.dk.
d)Electronic mail: peter.daivis@rmit.edu.au.

boundary condition has no theoretical foundation, and that although slippage may be present at macroscopic scale, it usually has negligible effect on the flow characteristics. At the nanoscale, however, we deal with nanolitre volumes of fluids in applications such as drug delivery and nanofiltration. Under these small flows slip can have a significant effect on the flow rate, so precise quantification and control of the fluid is required and hence the effect of slip becomes very important. The general boundary condition is often formulated using a quantity called the slip length, which is defined as the distance between the innermost solid surface and the plane away from the solid, where the tangent to the fluid velocity value matches that of the solid velocity. When the slip length is comparable to the channel size, the permeability of the channel increases by a significant amount which can have many potential advantages. The slip length is used to determine flow enhancement, defined as the ratio of the observed flow rate (in simulation or experiment) to that predicted from classical hydrodynamics with no slip boundary condition. For example, a slip length of about 60 nm (water on graphene) in a 10 μm channel has no measurable effect on the flux, but in a 10 nm channel, the flux is enhanced by 37 times.

For a considerable time slip has been a controversial subject,[9,15] but now it is well established that a liquid can slip on a solid surface in contact with it, i.e., the no-slip boundary condition is indeed violated. However, the data for the slip length is scattered both in experiments and simulations and the precise quantification of the slip length is a subject of great interest.

The general boundary condition reads

$$u_s = L_s \left.\frac{\partial u_x}{\partial y}\right|_{y=y_w}, \tag{1}$$

where u_s is the slip velocity (i.e., the relative tangential velocity between fluid and solid) and $\partial u_x/\partial y$ is the strain rate at the wall, assuming the fluid is confined in the y direction and the flow is in the x direction.

Navier first formulated the slip boundary condition,[16] which relates the slip velocity to the fluid-solid interfacial friction coefficient,

$$u_s = \frac{\eta_0}{\zeta_N} \left.\frac{\partial u_x}{\partial y}\right|_{y=y_w}, \tag{2}$$

such that the slip length is defined as

$$L_s = \frac{\eta_0}{\zeta_N}, \tag{3}$$

where η_0 is the shear viscosity of the fluid and ζ_N is the friction coefficient which is intrinsic to the fluid and solid system. Here the slip length is assumed to be constant, i.e., independent of the applied field or shear rate; however, we note that it has been shown to increase rapidly at high shear rates.[17,18]

The boundary condition is a property of the combined fluid-solid system and many other factors. Slip has been studied extensively using simulations, theory and experiments, but still the fundamental mechanism underlying slip is not clear and there are many open questions as it depends on various parameters in a very complex way. Refer to the reviews on slip and the references therein.[9,15,19,20] In simulations, slip can be quantified in two different ways. The widely used method is direct nonequilibrium molecular dynamics simulations (NEMD) simulations. For example, in a Poiseuille flow, the tangent to the fluid velocity at the wall is extrapolated from the wall to the position where it is equal to zero. In Couette flow, the simple linear velocity profile is extrapolated to match that of the wall velocity. Both of these NEMD methods use Eq. (1) to calculate the slip length. Due to the few nanoseconds of limited simulation times, NEMD simulations are generally done at high shear rates in Couette flow (or equivalently, field strengths in the case of Poiseuille flow) to generate reliable velocity profiles, i.e., to have satisfactory signal to noise ratio within the available computational time. This is possible only if the mean streaming velocities are comparable with the thermal velocity of the fluid due to the temperature. Water has a thermal velocity of about 340 m/s at room temperature, but fluid velocities in real experiments are just a few cm/s. The NEMD shear rates are therefore orders of magnitude higher than the shear rates we use in experimental studies and applications.[15] As mentioned above, slip is found to be constant at low shear rates, but increases rapidly and diverges at high shear rates. One should therefore be careful when interpreting the NEMD slip lengths, which are computed at a particular shear rate. Hence, to find out the limiting or minimum slip length for a given fluid-solid interface, one must perform NEMD simulations at various shear rates and extrapolate the results to experimental shear rates, which may also result in large statistical errors in the case of high slip systems. This is a cumbersome process and clearly necessitates an alternative method to quantify the slip, which should be tested for a variety of fluid and solid materials.

Another less commonly used method is equilibrium molecular dynamics simulations (EMD), where one calculates the friction coefficient between solid and fluid, and then uses the simple ratio of viscosity to the friction coefficient to give the slip length using Eq. (3). This method overcomes the limitations of NEMD methods and different methods have been applied to quantify the friction from EMD simulations.[1,21–23]

Slip depends on various parameters such as the nature of the wall and fluid, interaction strength between them, structure and pattern of the wall, density of fluid and surface density of wall, wetting properties, contact angle of the fluid on the surface, temperature, and viscosity of the fluid. Reviews on slip dependence on various parameters can be found in Refs. 9, 15, 19, and 20. Decoupling these factors from one another is not a feasible way to study their individual effects. Moreover, counter to intuition some of these studies found increasing slip with increasing surface roughness, decreasing slip with increasing contact angle on hydrophobic surfaces, and constant slip length at high shear rates, etc. making slip a very complex phenomenon requiring greater study.

We now briefly discuss the special properties of graphene surfaces which affect slip. In general, as the interaction strength between fluid and wall is decreased, slip increases.[17] Slip also increases with increasing the fluid contact angle on the wall surface (nonwetting),[15] and as surface density (incommensurability) of the wall increases, slip also increases.[17] Atomically smooth walls are also shown to produce larger

slip due to the small corrugations of the wall potential along the channel.[35] Graphene possesses all these characteristics. (i) The interaction strength between fluid atoms is stronger than that between fluid and carbon atoms, which makes the fluid recede from the wall and induces a high contact angle. (ii) The surface density of graphene is $\rho\sigma^2 = 5.54$, which is much higher than the fluid density and usual molecular walls (0.8–1.2) studied in simulations. (iii) The very strong covalent bonds between the carbon atoms in the graphene layer makes it very smooth. Therefore fluids in graphene nanochannels are expected to show high slip. Currently there is a lot of interest in the research community and industry to devise nanoengineered channels for various fluids to exhibit large and controlled slip,[24] so this matter is worth further investigation.

Due to the high surface density of carbon walls and the complexity of carbon potential models, most of the simulations of fluid flows in carbon nanochannels have used rigid walls (carbon atoms are fixed to their lattice sites) to decrease the simulation times, and to maintain a desired temperature the fluid is thermostated. Sokhan *et al.*[25] performed NEMD simulations of methane in flexible graphene nanochannels and found a 20% increase in the flux compared to using rigid walls. In a very recent study, Bernardi *et al.*[26] found that fixing the wall atoms and thermostating the fluid can induce severe artefacts for nanoflows. Furthermore, Martini *et al.*[27] found that the transport of momentum between fluid and wall is very important in determining the nanofluidic properties, thus rigid and nonrigid walls are expected to result in different fluidic behaviour.

III. METHODOLOGY

A. The fluid-solid friction coefficient

Here we briefly summarize the idea behind the method presented by Hansen *et al.*[1] and the final expressions for the quantities of interest. The reader is referred to the original paper for full details. Assume that a fluid is confined between two parallel walls with positions at $y_w = 0$ (wall 1) and $y_w = L_y$ (wall 2), respectively, along the y direction. We consider a fluid element with constant mass, m, and average volume $V = L_x \Delta L_z$, that is, a fluid slab adjacent to wall 1 and of average width Δ, which is about one molecular diameter (see Fig. 1). The fluid may be subjected to a constant external force per unit mass F_e in the x direction. The equation of motion of the slab is given by Newton's second law, i.e.,

$$m\frac{du_{\text{slab}}}{dt} = F_x'(t) + F_x''(t) + mF_e \,, \tag{4}$$

where u_{slab} is the center of mass velocity of the slab (adjacent to wall 1) in the x direction, F_x' is the force due to wall-slab interactions, and F_x'' is the force due to fluid-slab interactions.

The wall-slab force term, F_x', can be viewed as a frictional shear force that depends on the relative velocity between the wall and the fluid. For sufficiently small relative velocities one may then propose the following linear constitutive equation relating the wall-slab shear force to the velocity difference, $\Delta u' = u_{\text{slab}} - u_w$,

$$F_x'(t) = -\int_0^t \zeta(t-\tau)\Delta u'(\tau)\,d\tau + F_r'(t) \,, \tag{5}$$

where ζ is a friction kernel. F_r' is a random force term with zero mean that is assumed to be uncorrelated with u_{slab}. For steady flows the time average of Eq. (5) is given by

$$\langle F_x' \rangle = -\zeta_0 \left\langle \Delta u' \right\rangle \,, \tag{6}$$

where ζ_0 is the zero frequency friction coefficient multiplied with the surface area of the solid wall. It is worth noting that Eq. (5) is a local relation, i.e., the kernel ζ depends only on the force between the slab and the wall.

In order to account for the fluid-slab shear force, F_x'', one can apply Newton's law of viscosity. Thus, for steady flows we have

$$\langle F_x'' \rangle = A\eta_0 \langle \dot{\gamma} \rangle = A\eta_0 \left.\frac{\partial u}{\partial y}\right|_{y=\Delta} \,, \tag{7}$$

where $A = L_x L_z$ is the surface area of the slab. For $u_w = 0$, Eq. (5) is written as

$$F_x'(t) = -\int_0^t \zeta(t-\tau) u_{\text{slab}}(\tau)\,d\tau + F_r'(t) \,. \tag{8}$$

Multiplying both sides by $u_{\text{slab}}(0)$ and taking the ensemble average it is possible to form the corresponding relation between the slab velocity-force cross correlation function (CCF) $C_{uF_x'}(t)$ and the slab velocity autocorrelation function (ACF) $C_{uu}(t)$

$$C_{uF_x'}(t) = -\int_0^t \zeta(t-\tau) C_{uu}(\tau)\,d\tau \tag{9}$$

such that

$$\begin{aligned} C_{uF_x'}(t) &= \langle u_{\text{slab}}(0) F_x'(t) \rangle \quad \text{and} \\ C_{uu}(t) &= \langle u_{\text{slab}}(0) u_{\text{slab}}(t) \rangle \,. \end{aligned} \tag{10}$$

One can compute the above two correlation functions using EMD simulations following Ref. 1. We Laplace transform Eq. (9) to a more convenient form,

$$\widetilde{C}_{uF_x'}(s) = -\widetilde{\zeta}(s)\,\widetilde{C}_{uu}(s) \,. \tag{11}$$

The above two correlation functions can be related by assuming a Maxwellian function, which in Laplace space takes the form,

$$\widetilde{C}_{uF_x'}(s) = -\sum_{i=1}^{n} \frac{B_i\,\widetilde{C}_{uu}(s)}{s+\lambda_i} \,, \tag{12}$$

thus ζ_0 can be found via the fitting parameters,

$$\zeta_0 = \int_0^\infty \sum_{i=1}^{n} B_i\, e^{-\lambda_i t}\,dt = \sum_{i=1}^{n} B_i/\lambda_i \,. \tag{13}$$

Finally, the fluid-solid intrinsic interfacial friction coefficient ξ_0, can be found by dividing ζ_0 by the surface area of the confining solid wall A,

$$\xi_0 = \zeta_0 / A. \tag{14}$$

B. Derivation of the slip length

For steady flows, and by using integral boundary conditions (IBCs), it is possible to solve the Navier-Stokes equation

in terms of the slab center of mass velocity, u_{slab}. In this way we also obtain an equation for the strain rate at $y = \Delta$. From Eq. (4) we can then express u_{slab} as a function of the friction coefficient ζ_0 using Eqs. (6) and (7). This finally leads to an explicit equation for the slip length using Eq. (1). Again, for details we refer to Hansen *et al.*[1]

1. Planar Couette flow

Consider a planar Couette flow with identical walls. For wall 1 at rest and wall 2 with velocity u_w, solving the Navier-Stokes equation using the appropriate IBCs leads to the slip coordinate,

$$L = -u(0) \Big/ \left.\frac{\partial u}{\partial y}\right|_{y=0} = \frac{\Delta}{2} - \frac{\eta_0}{\xi_0}\,. \tag{15}$$

The absolute value of this slip coordinate is the slip length and in the limit of zero slab width, $\Delta \to 0$, we obtain the slip length $L_s = \eta_0/\xi_0$ in accordance with the Navier slip length, Eq. (3). The average slab center of mass velocity at wall 1 is then given by

$$\langle u_{\text{slab}} \rangle = \frac{\eta_0 u_w}{\xi_0(L_y - \Delta) + 2\eta_0}. \tag{16}$$

2. Planar Poiseuille flow

If an external force per unit mass, F_e, is applied to the fluid and both walls are at rest, the Navier-Stokes equation with the appropriate IBCs leads to the slip coordinate

$$L = \Delta\left(\frac{1}{2} - \frac{\Delta}{3L_y}\right) - \frac{\eta_0}{\xi_0}\,, \tag{17}$$

which means that $L_s = \eta_0/\xi_0$ as $\Delta \to 0$ as expected. The average slab center of mass velocity for this flow is given by

$$\langle u_{\text{slab}} \rangle = \frac{\rho F_e L_y}{2\xi_0}\,. \tag{18}$$

It is important to note here that the slip length from Eq. (17) is different from Eq. (15) by the term $-\Delta^2/3L_y$. Since L_y is typically significantly larger than the width of the interfacial region, Δ, the effect of this term cannot be measured using direct NEMD within statistical errors. Therefore both Poiseuille and Couette flow slip lengths are practically identical and equal to the Navier slip length as $\Delta \to 0$.

IV. SIMULATION DETAILS

The molecular dynamics simulations are carried out using standard techniques.[10,28,29] The reliability of any simulation depends among other things on the accuracy of the potentials applied. As mentioned above, in nanofluidic systems the wall-fluid interactions become as important as the fluid-fluid interactions, whereas at the macroscale the wall has no effect on the hydrodynamic properties of the fluid, other than just confining the fluid and providing the boundary condition for the velocity. Here we model graphene using the second generation reactive empirical bond order Tersoff-Brenner potential (REBO), which is widely used for graphene/carbon nanotube structures.[30] It is parameterised using quantum mechanical calculations and it describes the mechanical properties, elastic properties and dynamics of covalently bonded carbon atoms accurately.[31] The bond strength between two carbon atoms also depends on the neighbouring atoms and the bond environment and can be written as

$$E_b = \sum_i \sum_{j(>i)} [V^R(r_{ij}) - b_{ij} V^A(r_{ij})]\,, \tag{19}$$

where r_{ij} is the distance between particles i and j. The terms $V^R(r_{ij})$ and $V^A(r_{ij})$ are pair additive interactions that represent interatomic repulsions and attraction, respectively. The term b_{ij} is called the bond order term and it incorporates the bond environment, coordination number, bond angle, and dihedral angle with its covalently bonded neighbouring carbon atoms.

The interactions between the fluid-fluid and fluid-wall atoms are modelled using the standard Lennard-Jones potential

$$\phi = \sum_i \sum_{j(>i)} 4\epsilon \left[\left(\frac{\sigma}{r_{ij}}\right)^{12} - \left(\frac{\sigma}{r_{ij}}\right)^{6}\right], \tag{20}$$

where ϵ and σ are the interaction strength and the length scale, respectively. The interaction cutoff is set to 1 nm. To maintain the stability of the system we have used two layers of graphene at each wall. The separation of the two layers is kept at 0.34 nm using the Lennard-Jones potential acting between carbon atoms belonging to different layers, and the centre of mass of each graphene layer is then kept fixed to avoid drift.

The simulated state points and the interaction parameters are listed in Table I. The fluid-carbon interaction parameters are derived using the Lorentz-Berthelot rule. A Nosé-Hoover thermostat[32,33] is applied to the wall atoms to maintain a desired temperature, so the viscous heating generated by the fluid is transmitted to and conducted through the walls as is done in a real experimental system. The equations of motion for all particles were integrated forward in time using a leap-frog integration scheme with time step $\Delta t = 1$ fs. The very strong covalently bonded interactions between carbon atoms demands a relatively small time step for the integration scheme. The system's dimensions along the x and

TABLE I. Interaction parameters, fluids state point under study and results. For density and temperature the values inside the parentheses are corresponding standard reduced molecular dynamics units. Note: for carbon $\sigma = 0.34$ nm and $\epsilon/k_B = 28$ K.

Fluid	σ_{ff} (nm)	ϵ_{ff}/k_B (K)	σ_{fw} (nm)	ϵ_{fw}/k_B (K)	ρ (kg m^{-3})	T (K)	$\eta/10^{-5}$ (Ref. 37) (kg m^{-1} s^{-1})	$\xi/10^4$ (kg m^{-2} s^{-1})	L_s (nm)
Ar	0.34	120.0	0.34	57.96	1361.8(0.8)	120.0(1)	17.7 ± 1.7	1.62 ± 0.04	11 ± 1
CH_4	0.38	148.1	0.36	64.39	387.6(0.8)	148.1(1)	9.9 ± 0.9	1.67 ± 0.04	6 ± 0.6

z directions are $L_x = 3.44$ nm and $L_z = 3.4$ nm and the distance between the two innermost graphene layers along the confinement direction is $L_y = 5.1$ nm so the full system size in the y direction is 5.78 nm. Periodic boundary conditions are imposed along the x and z directions. All simulation results are averaged over 20 independent simulations which run from 10 to 30 $\times$ 10^6 time steps depending on the shear rate and external field. For fluids in very smooth channels, such as graphene, simulations require a long time.[25]

V. RESULTS AND DISCUSSION

First we begin with the EMD simulations, where the confined fluid is at equilibrium. The friction between solids can be viewed as the shearing force between two surfaces in contact with each other. Similarly the hydrodynamic friction can also be viewed as the shearing force between the solid surface and the first fluid layer in contact with the solid surface. Niavarani *et al.*[34] quantified the slip length using the structure and density of the first fluid layer close to the wall. We choose a fluid slab of average slab width about one molecular diameter and constant mass adjacent to the wall.[1] After equilibration, the total wall-slab shearing force is evaluated directly via

$$F_x'(t) = \sum_{\substack{i \in \text{slab} \\ j \in \text{wall}}} F_{ij,x}(t)\,, \tag{21}$$

where $F_{ij,x}$ is the force in the x direction on slab particle i due to wall particle j at time t. Similarly the x component of the center of mass velocity of the slab is calculated via

$$u_{\text{slab}}(t) = \frac{1}{m} \sum_{i \in \text{slab}} m_i v_{i,x}(t)\,, \tag{22}$$

where $v_{i,x}$ is the velocity of slab particle i and $m = \sum_{i \in \text{slab}} m_i$. From these two quantities, we evaluate the correlation functions $C_{uF_x'}(t)$ and $C_{uu}(t)$. In Fig. 2 we show an example of normalized slab velocity ACF $C_{uu}(t)$ and slab velocity-force CCF $C_{uF_x'}(t)$ for CH_4. The slab velocity and force are anti-correlated to each other, since the shearing force on the fluid slab due to the adjacent wall acts in the direction opposite to the flow. The correlation function data are then Laplace transformed according to the method described above, and an example is given in Fig. 3. Note, Fig. 3(b) also includes the Maxwellian fit ($n = 1$) to the transformed correlation functions, Eq. (12). The friction coefficient is then evaluated by using the fitting parameters and the surface area of graphene using Eqs. (13) and (14).

The slip length is directly calculated using this friction coefficient and the shear viscosity of the fluid Eq. (3). Our EMD simulations thus predict slip lengths for argon and methane of 11 ± 1 nm and 5.9 ± 0.6 nm, respectively, with the corresponding friction coefficients $(1.62 \pm 0.04) \times 10^4$ kg m^{-2} s^{-1} and $(1.67 \pm 0.04) \times 10^4$ kg m^{-2} s^{-1}. Here note that the fluids are at different state points and the size and interaction strength of methane is slightly higher than that of argon, see Table I.

To compare our EMD model predictions with the standard NEMD, we carried out both Poiseuille and Couette flow simulations. In Poiseuille flow, each fluid atom is acted upon by an external body force and in Couette flow the upper graphene wall is moved at a constant velocity while the lower wall is held fixed. We have carried out these simulations for a wide range of external fields and shear rates to capture both the constant and diverging behaviour of the slip length. In Poiseuille flow, the smallest field we used results in a mean fluid velocity around 2 m/s and in Couette flow we move the upper graphene layer with velocity as small as 5 m/s. Below these fields and shear rates the velocity profiles are too noisy to extract useful data. Note that these low fields and shear rates are an order of magnitude smaller than typical values used in NEMD simulations.[15] During NEMD simulations, fluid velocity, density, and temperature profiles are evaluated by dividing the channel into bins of 0.1 nm width. The fluid density and temperature profiles are not presented here.

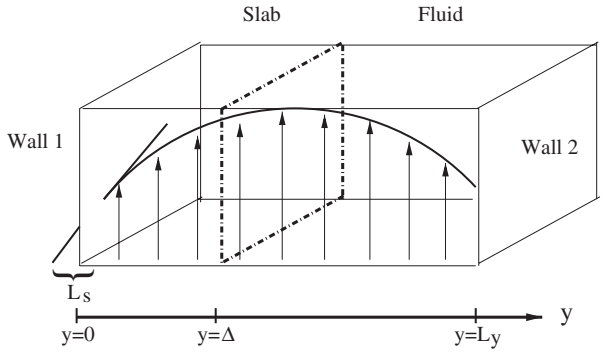

FIG. 1. Schematic illustration of the system. The arrows inside the box indicate the velocity field forming the profile. L_s is the slip length and Δ is the slab width, typically, about one molecular diameter of the fluid. The width of the channel is L_y. Image reprinted with permission from J. S. Hansen, B. D. Todd, and P. J. Daivis, Phys. Rev. E **84**, 016313 (2011). Copyright 2011 by the American Physical Society.

The Poiseuille flow velocity profiles are fitted to a quadratic fit, i.e., $u_x(y) = ay^2 + b$ whereas the Couette flow profiles are fit to a linear function, i.e., $u_x(y) = ay + b$. From these fits we can calculate the slip velocity and velocity gradient at the wall, and hence the NEMD slip lengths from Eq. (1).

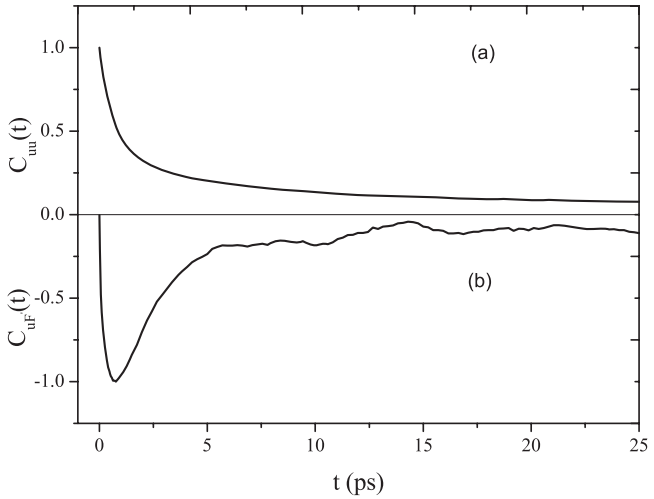

FIG. 2. Section of the normalized correlation functions (a) C_{uu} and (b) $C_{uF_x'}$ versus time for CH_4.

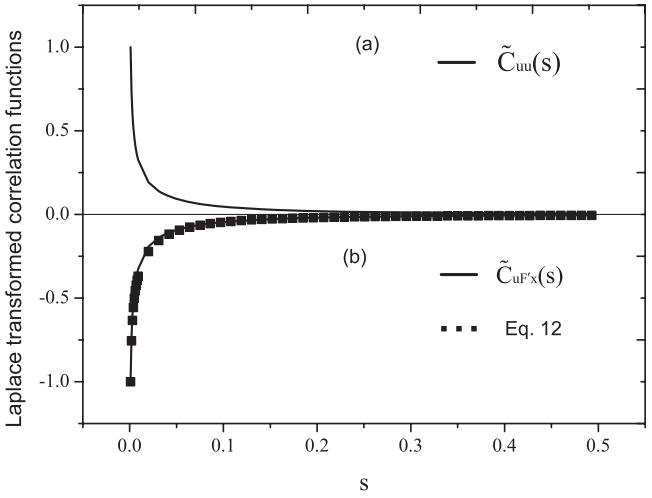

FIG. 3. Normalized Laplace transform of the correlation functions (a) C_{uu} and (b) $C_{uF_x'}$ shown in Fig. 2. Note that (b) also includes the Maxwellian fit, Eq. (12). For clarity we have removed some of the fitting data points.

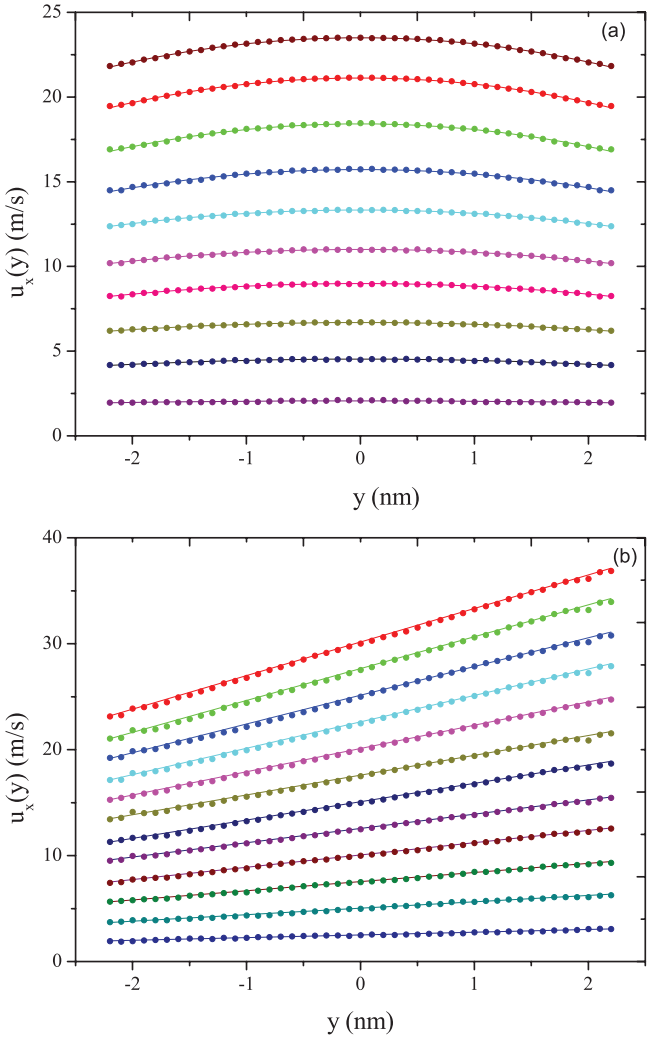

FIG. 4. Streaming velocity profiles (a) Poiseuille flow of argon (b) Couette flow of methane. Points are NEMD data and continuous lines are corresponding fits. In Poiseuille flow external fields are 0.1×10^{11} to 1.0×10^{11} m/s^2 with an increment of 0.1×10^{11} m/s^2 (bottom to top). In Couette flow upper wall velocities are 5 to 60 m/s with an increment of 5 m/s (bottom to top).

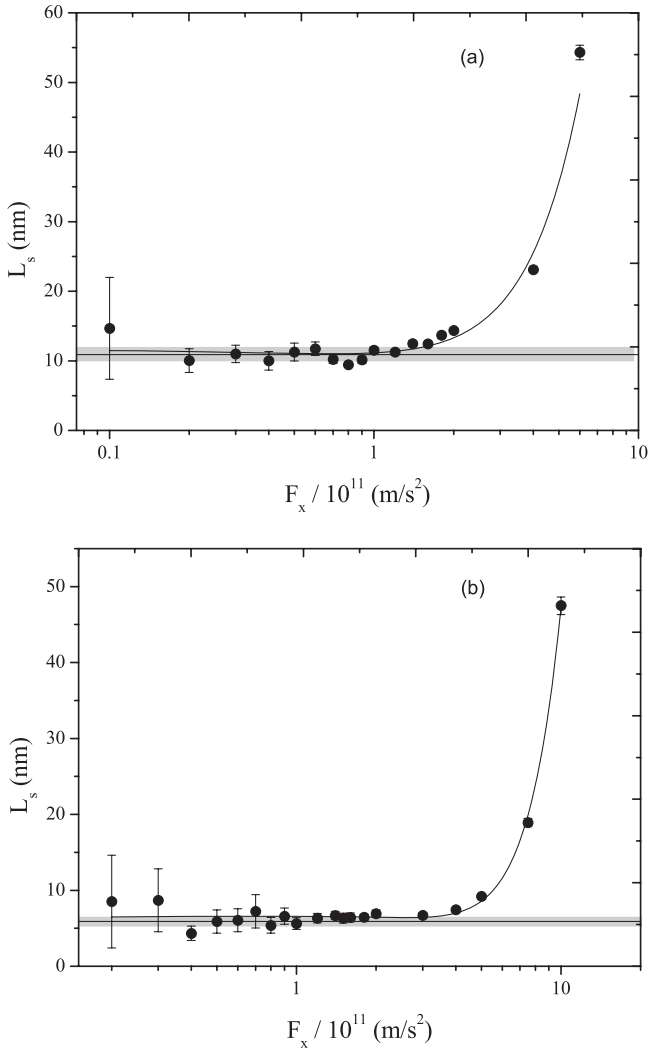

FIG. 5. Slip length as a function of external field in Poiseuille flow for (a) argon and (b) methane. The straight line is prediction from EMD (Eq. (3)) and the shaded region is the standard error in EMD.

In Fig. 4 we plot the Poiseuille flow velocity profiles of argon and the Couette flow velocity profiles of methane along with their corresponding fits. As can be seen, the fluid has a significant velocity at the wall compared to its mean velocity in the Poiseuille flow. In the Couette flow one can see the finite velocity difference between the fluid velocity at the wall and the wall velocity. These indicate significant slip is occurring in both systems.

In Fig. 5 we plot the slip length of argon and methane as a function of the external field along with our EMD predicted L_s, which is a constant. As can be seen from the figures at low fields, the slip length is constant and is in excellent agreement with our EMD prediction before it diverges at high fields. In Fig. 6 the slip length of argon and methane is shown as a function of the upper wall velocity (shear rate can be found by dividing the wall velocity with the channel width) along with our EMD predicted slip length L_s. Again, as can be seen from the figures, at low shear rates the slip length is constant and is in excellent agreement with our EMD prediction before it diverges at high shear rates.

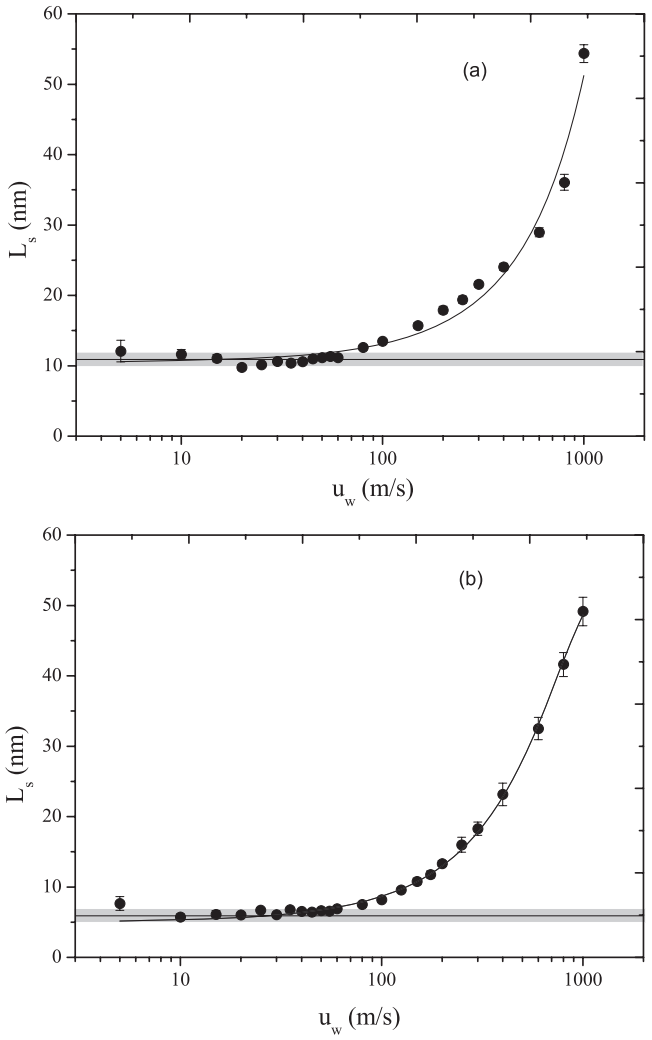

FIG. 6. Slip length as a function of shear rate in Couette flow for (a) argon and (b) methane. The straight line is prediction from EMD (Eq. (3)) and the shaded region is the standard error in EMD.

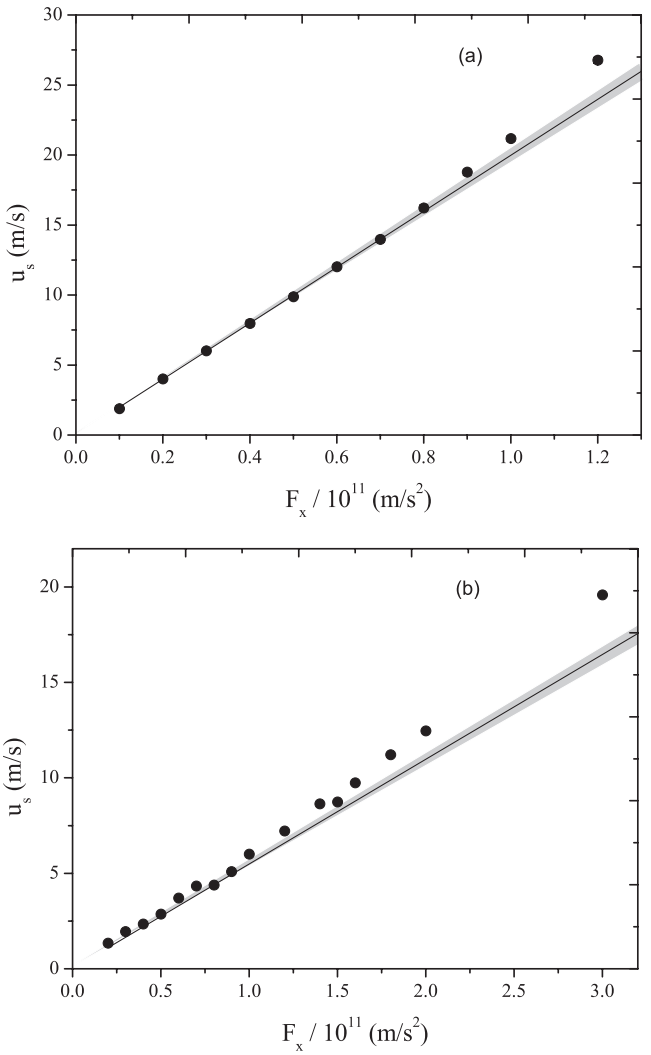

FIG. 7. Comparison of slip velocity predicted from EMD (Eq. (18)) (straight line) and direct NEMD (points) as a function of external field in Poiseuille flow for (a) argon and (b) methane. The shaded region is the standard error in EMD and the standard error in NEMD data is smaller than the symbol size.

Both the Poiseuille and Couette flow NEMD slip lengths are found to be equal and are in excellent agreement with our EMD based friction model. Our results convincingly demonstrate that one can avoid the cumbersome NEMD methods to calculate the limiting slip length for a given fluid-solid combination by using our method, thus saving enormous amounts of central processing unit times (the computational time required to calculate the friction coefficient from the EMD method is equal to the time required to generate just one NEMD data point on Fig. 5 or 6).

In the literature, various researchers have found constant, increasing, decreasing, and nonlinear slip behaviour for different systems as the shear rate is increased. Thompson *et al.*[17] found a constant slip length below a critical shear rate and diverging slip length above the critical shear rate. Priezjev *et al.*[35] found linearly increasing slip length with shear rate, while Niavarani *et al.*[34] found nonlinear variation of the slip length with shear rate. Martini *et al.*[27] found a constant slip length at high shear rates, and using atomic force microscopy Zhu *et al.*[8] found a nonlinear behaviour of slip for different fluids. We refer to the original papers, reviews,[9,15,19,20] and the references therein for more details. These results suggest that the behaviour of slip due to the changes in applied shear rate is nontrivial. A shear rate $\dot{\gamma}_l$ which corresponds to limiting slip length for a fluid-solid system may not result in limiting slip length for other systems. The maximum shear rates which correspond to the limiting slip length in this study are smaller than the shear rates which resulted in limiting slip length in our previous study of the same fluid with molecular Lennard-Jones walls, where the slip length is an order of magnitude smaller than the slip length found here. Water on the same graphene surface, which is currently under study,[36] is expected to show even higher slip, hence even smaller shear rates should be used to find the limiting slip length using NEMD simulations. For CH_4 and H_2O confined in molecular crystal walls (LJ) and graphene surfaces (C), we have $\dot{\gamma}_{l(CH_4-LJ)} > \dot{\gamma}_{l(CH_4-C)} > \dot{\gamma}_{l(H_2O-C)}$. Thus if one has to predict the limiting slip length from NEMD simulations, several shear rates should be used and the dynamical behaviour of slip has to be examined to quantify the limiting slip length as one does not know the shear rate which corresponds to the

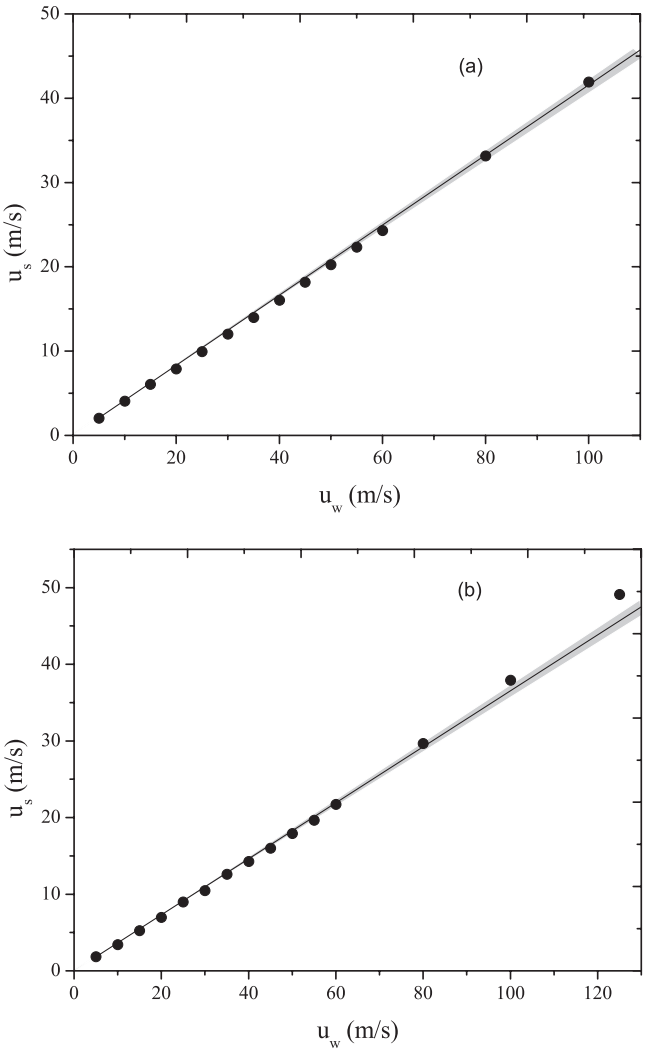

FIG. 8. Comparison of slip velocity predicted from EMD (Eq. (16)) (straight line) and direct NEMD (points) as a function of wall velocity in Couette flow for both (a) argon and (b) methane. The shaded region is the standard error in EMD and the standard error in NEMD data is smaller than the symbol size.

limiting slip length *a priori*. On the other hand, EMD methods such as ours can predict the limiting low velocity slip from a single simulation, making it a far more appealing and reliable method.

We further predict the slip velocities from our model using Eqs. (16) and (18) and compare them with the direct NEMD data. In Fig. 7 we plot the slip velocity of argon and methane as a function of the external field, along with our model prediction for Poiseuille flow. As can be seen from the figures in the linear regime the predicted slip velocities are in excellent agreement with the direct NEMD slip velocities. In Fig. 8 we plot the slip velocity of argon and methane as a function of the shear rate, along with our model prediction for Couette flow. Again as can be seen from the figures in the linear regime the predicted slip velocities are in excellent agreement with the direct NEMD slip velocities.

All the NEMD streaming velocity profiles in Fig. 4 result in constant slip length and the slip velocities are in agreement with their corresponding EMD predictions. Above these shear rates nonlinear effects begin to start and the results show deviations from our model predictions, as expected.

As explained earlier, several properties of graphene contribute to the observed slip and the slip lengths are higher than the channel's width which significantly influences the nanofluidic behaviour. To our knowledge this is the first time that the EMD predicted slip length is compared in both Poiseuille and Couette flow NEMD simulations for a wide range of external fields and shear rates, respectively.

As far as we are aware there have been no experimental studies done on methane slip confined to graphene nanochannels. Our only point of comparison is with the simulation studies of Sokhan *et al.*[25] Their fluid state point (density and temperature) is different from ours and their external field strength is also higher. Nevertheless their slip length varied between 2 to 10 nm, while our slip length is around 6 nm.

VI. CONCLUSION

Using extensive molecular dynamics simulations of methane and argon flowing in graphene nanochannels we examined the hydrodynamic boundary condition. The no-slip boundary condition is shown to be violated for fluids confined by graphene surfaces owing to their atomic smoothness and lyophobicity. The friction coefficient between the fluids studied here and graphene is found to be an order of magnitude smaller than the friction between the same fluids and the molecular Lennard-Jones crystal walls generally employed in computer simulations. In nanoscale fluidic systems the boundary condition is a combined property of both fluid-fluid and fluid-solid interactions. Slip is shown to be independent of the flow type, confirming its intrinsic nature. Our EMD method is shown to be both computationally highly efficient and superior in predicting the slip compared to the conventional NEMD methods of estimating slip. Our EMD method computes the limiting or minimum slip length for a given fluid and solid surface without the need to do cumbersome NEMD simulations for various shear rates or external fields and their extrapolation to experimental conditions. We note that care should be taken when interpreting the NEMD slip length as it may not correspond to the limiting slip length. Using our method one can also predict the slip velocity of the fluid near the solid surface. Flow rates are found to be an order of magnitude higher compared to classical hydrodynamic no-slip boundary condition predictions, which is very important in reducing the friction in lubrication applications and enhancing the flow rates to design novel nonofluidic devices. Studies with more complex fluids such as water using our newly devised model are currently under study.

ACKNOWLEDGMENTS

This project was supported by the Victorian Partnership for Advanced Computing HPC Facility and Support Services and an award under the Merit Allocation Scheme on the NCI National Facility at the ANU. J. S. Hansen wishes to acknowledge Lundbeckfonden for supporting this work as a part of Grant No. R49-A5634.

[1]J. S. Hansen, B. D. Todd, and P. J. Daivis, Phys. Rev. E **84**, 016313 (2011).
[2]R. B. Schoch, J. Han, and P. Renaud, Rev. Mod. Phys. **80**, 839 (2008).
[3]J. C. T. Eijkel and A. v. d. Berg, Microfluid. Nanofluid. **1**, 249 (2005).
[4]L. Bocquet and E. Charliax, Chem. Soc. Rev. **39**, 1073 (2010).
[5]W. Sparreboom, A. v. d. Berg, and J. C. T. Eijkel, New J. Phys. **12**, 015004 (2010).
[6]K. P. Travis, B. D. Todd, and D. J. Evans, Phys. Rev. E **55**, 4288 (1997).
[7]K. P. Travis and K. E. Gubbins, J. Chem. Phys. **112**, 1984 (2000).
[8]Y. Zhu and S. Granick, Phys. Rev. Lett. **88**, 106102 (2002).
[9]C. Neto, D. R. Evans, E. Bonaccurso, H.-J. Butt, and V. S. J. Craig, Rep. Prog. Phys. **68**, 2859 (2005).
[10]M. P. Allen and D. J. Tildesley, *Computer Simulation of Liquids* (Clarendon, New York, 1987).
[11]D. Frenkel and B. Smit, *Understanding Molecular Simulation* (Academic, London, 1996).
[12]S. Han, M. Y. Choi, P. Kumar, and H. E. Stanley, Nat. Phys. **6**, 685 (2010).
[13]B. D. Todd and J. S. Hansen, Phys. Rev. E **78**, 051202 (2008).
[14]B. D. Todd, J. S. Hansen, and P. J. Daivis, Phys. Rev. Lett. **100**, 195901 (2008).
[15]E. Lauga, M. P. Brenner, and H. A. Stone, *Experimental Fluid Dynamics* (Springer, New York, 2007).
[16]C. L. M. H. Navier, Mem. Acad. Sci. Inst. Fr. **6**, 389 (1823).
[17]P. A. Thompson and M. O. Robbins, Nature (London) **389**, 360 (1997).
[18]Y. Zhu and S. Granick, Phys. Rev. Lett. **87**, 096105 (2001).
[19]L. Bocquet and J.-L. Barrat, Soft Matter **3**, 685 (2007).
[20]B.-Y. Cao, J. Sun, M. Chen, and Z.-Y Guo, Int. J. Mol. Sci. **10**, 4638 (2009).
[21]L. Bocquet and J.-L. Barrat, Phys. Rev. E **49**, 3079 (1994).
[22]V. P. Sokhan and N. Quirke, Phys. Rev. E **78**, 015301R (2008).
[23]J. Petravic and P. Harrowell, J. Chem. Phys. **127**, 174706 (2007); Erratum **128**, 209901 (2008).
[24]J. C. T. Eijkel, Lab Chip **7**, 299 (2007).
[25]V. P. Sokhan, D. Nicholson, and N. Quirke, J. Chem. Phys. **115**, 3878 (2001).
[26]S. Bernardi, B. D. Todd, and D. J. Searles, J. Chem. Phys. **132**, 244706 (2010).
[27]A. Martini, H.-Y. Hsu, N. A. Patankar, and S. Lichter, Phys. Rev. Lett. **100**, 206001 (2008).
[28]D. J. Evans and G. P. Morriss, *Statistical Mechanics of Nonequilibrium Liquids* (Academic, New York, 1990).
[29]B. D. Todd, D. J. Evans, and P. J. Daivis, Phys. Rev. E. **52**, 1627 (1995).
[30]D. W. Brenner, O. A. Shenderova, J. A. Harrison, S. J. Stuart, B. Ni, and S. B. Sinnott, J. Phys. Condens. Matter **14**, 783 (2002).
[31]H. Rafii-Tabar, *Computational Physics of Carbon Nanotubes* (Cambridge University Press, New York, 2008).
[32]S. Nosé, Mol. Phys. **52**, 255 (1984).
[33]W. G. Hoover, Phys. Rev. A **31**, 1695 (1985).
[34]A. Niavarani and N. V. Priezjev, Phys. Rev. E **77**, 041606 (2008).
[35]N. V. Priezjev, J. Chem. Phys. **127**, 144708 (2007).
[36]S. K. Kannam, B. D. Todd, J. S. Hansen, and P. J. Daivis, "Slip length of water on graphene: Limitations of non-equilibrium molecular dynamics simulations" (unpublished).
[37]R. L. Rowley and M. M. Painter, Int. J. Thermophys. **18**, 1109 (1997).